HHS Public Access

Author manuscript

Clin Cancer Res. Author manuscript; available in PMC 2020 May 01.

Published in final edited form as:

Clin Cancer Res. 2019 November 01; 25(21): 6452–6462. doi:10.1158/1078-0432.CCR-19-0799.

Glycogen Synthase Kinase-3 Inhibition Sensitizes Pancreatic Cancer Cells to Chemotherapy by Abrogating the TopBP1/ATR-Mediated DNA Damage Response

Li Ding[1], **Vijay S. Madamsetty**[2], **Spencer Kiers**[1], **Olga Alekhina**[1], **Andrey Ugolkov**[3], **John Dube**[1], **Yu Zhang**[1], **Jin-San Zhang**[1,4], **Enfeng Wang**[2], **Shamit K. Dutta**[2], **Daniel M. Schmitt**[3], **Francis J. Giles**[3], **Alan P. Kozikowski**[5], **Andrew P. Mazar**[6], **Debabrata Mukhopadhyay**[2], **Daniel D. Billadeau**[1,7]

[1]The Division of Oncology Research, Schulze Center for Novel Therapeutics, Mayo Clinic, Rochester, MN, USA

[2]Department of Biochemistry and Molecular Biology, Mayo Clinic, Jacksonville, FL, USA

[3]Actuate Therapeutics Inc., Fort Worth, TX, USA

[4]Center for Precision Medicine, The First Affiliated Hospital of Wenzhou Medical University; Institute of Life Science, Wenzhou University, Zhejiang, China

[5]Starwise Therapeutics LLC, Madison, WI, USA

[6]Monopar Therapeutics Inc., Wilmette, IL, USA

Abstract

Purpose: Pancreatic ductal adenocarcinoma (PDAC) is a predominantly fatal common malignancy with inadequate treatment options. Glycogen synthase kinase 3β (GSK-3β) is an emerging target in human malignancies including PDAC.

Experimental Design: Pancreatic cancer cell lines and patient-derived xenografts were treated with a novel GSK-3 inhibitor 9-ING-41 alone or in combination with chemotherapy. Activation of the DNA damage response pathway and S-phase arrest induced by gemcitabine were assessed in pancreatic tumor cells with pharmacologic inhibition or siRNA depletion of GSK-3 kinases by immunoblotting, flow cytometry and immunofluorescence.

Results: 9-ING-41 treatment significantly increased pancreatic tumor cell killing when combined with chemotherapy. Inhibition of GSK-3 by 9-ING-41 prevented gemcitabine-induced S-phase arrest suggesting an impact on the ATR-mediated DNA damage response. Both 9-ING-41 and siRNA depletion of GSK-3 kinases impaired the activation of ATR leading to the

[7]Corresponding author: Daniel D. Billadeau, Ph.D., Billadeau.Daniel@mayo.edu; Division of Oncology Research and Schulze Center for Novel Therapeutics, Mayo Clinic, 200 First ST SW, Rochester, MN 55905.

Disclosure of Potential Conflicts of Interest: A. Ugolkov has equity interest in Actuate Therapeutics Inc. D.M. Schmitt is an employee of Actuate Therapeutics Inc. and has equity interest in Actuate Therapeutics Inc. F.J. Giles has equity interest in Actuate Therapeutics Inc. A.P. Kozikowski has equity interest in Actuate Therapeutics Inc. and is a co-inventor listed on the 9-ING-41 patent. A.P. Mazar has equity interest in Actuate Therapeutics Inc. D.D. Billadeau serves on the Scientific Advisory Board of Actuate Therapeutics Inc. and has equity interest in Actuate Therapeutics Inc. No potential conflicts of interest were disclosed by the other authors.

phosphorylation and activation of Chk1. Mechanistically, depletion or knockdown of GSK-3 kinases resulted in the degradation of the ATR-interacting protein TopBP1, thus limiting the activation of ATR in response to single-strand DNA damage.

Conclusions: These data identify a previously unknown role for GSK-3 kinases in the regulation of the TopBP1/ATR/Chk1 DNA damage response pathway. The data also support the inclusion of patients with PDAC in clinical studies of 9-ING-41 alone and in combination with gemcitabine.

Keywords

Pancreatic ductal adenocarcinoma; GSK-3β; DNA damage response; ATR; TopBP1

Introduction

Pancreatic ductal adenocarcinoma (PDAC), which constitutes 93% of pancreatic cancers, is predicted to be the second leading cause of cancer-related deaths in the USA by 2030 {1, 2}. The 5-year relative survival rate of all stages combined PDAC patients is less than 10% {3}. As a standard therapy for locally advanced and metastatic pancreatic cancer, gemcitabine has a 5.4% partial response rate {4} and the great preponderance of initially sensitive tumors develop overt chemoresistance within weeks {5}. FOLFIRINOX (folinic acid, fluorouracil, irinotecan, and oxaliplatin) and Nab-paclitaxel in combination with gemcitabine represent modest improvements over single agent gemcitabine {6, 7}. Novel approaches are thus urgently needed for patients with PDAC as are mechanism-based discovery of new therapeutic strategies to overcome chemotherapy resistance {8}.

Glycogen synthase kinase-3 (GSK-3) α and β are highly conserved serine-threonine kinases initially described as key enzymes in regulating glycogen metabolism, with critical roles in Wnt/β-catenin signaling, immune regulation, and maintenance of stem cell identity {9, 10}. We have previously shown that GSK-3β expression is regulated by oncogenic KRas signaling and its overexpression together with nuclear accumulation correlated with moderately and poorly differentiated pancreatic tumors {11-13}. We found that GSK-3β promoted cell proliferation and survival through the regulation of NFκB-dependent gene transcription {12}. Consistent with this growth promoting effect of GSK-3β in PDAC, pharmacologic inhibition or genetic depletion of GSK-3β limited pancreatic cancer cell viability *in vitro* and suppressed tumor growth *in vivo* {11, 14, 15}. Using a genetically engineered mouse model we demonstrated that GSK-3β contributes to KRas-driven tumor-promoting pathways that are required for the initiation of acinar-to-ductal metaplasia {16}. These data support the potential therapeutic benefit of targeting GSK-3 in human pancreatic cancer.

GSK-3 inhibitor tool compounds have been developed and tested for their abilities to sensitize pancreatic cancer cells to gemcitabine. Previous studies in hematopoietic cells {17} and pancreatic cancer cells {18} showed that activation of the Akt-GSK-3β pathway is a key signaling event for gemcitabine resistance. The GSK-3β inhibitor tool compound Bio {19} could prevent the sensitization to gemcitabine-induced cell death by zidovudine {18}. Lithium, a GSK-3 inhibitor, synergistically enhances the anti-cancer effect of gemcitabine

by promoting the ubiquitin-dependent proteasome degradation of Gli1 {20, 21}. The GSK-3 inhibitor AR-A014418 {22} also sensitizes pancreatic cancer cells to gemcitabine with altered expression of genes involved in DNA repair {23}. Interestingly, while GSK-3β inhibition could disrupt NFκB activity in pancreatic cancer cells it did not significantly sensitize these cells to gemcitabine {24}. The GSK-3 inhibitor LY2090314 {25} was clinically evaluated in patients for metastatic pancreatic cancer {} but its adverse PK properties ended its development. We have shown that a series of novel GSK-3 inhibitors, from which the clinical candidate, 9-ING-41 emerged, impaired PDAC and ovarian cancer cell proliferation and survival *in vitro* {26,27}, but its effects on PDAC *in vivo* and mechanism of action are not known.

Herein, we provide evidence that 9-ING-41, which is currently being evaluated in a phase 1/2 trial in patients with advanced cancer, reduces proliferation of PDAC cells *in vitro* and xenografts *in vivo*, and significantly sensitizes them to gemcitabine. 9-ING-41 impairs the ATR/Chk1 DNA damage response (DDR) signaling pathway induced by gemcitabine. Mechanistically, we show that pharmacologic inhibition or genetic depletion of GSK-3β led to the degradation of TopBP1, a key molecule that is required for optimal ATR phosphorylation of Chk1 leading to S-phase arrest and DNA repair. These data describe a previously unrecognized role for GSK-3β in regulating the ATR-Chk1 DDR pathway and provide a compelling rationale for the inclusion of patients with PDAC in clinical studies of 9-ING-41 in combination with gemcitabine/abraxane or MM398.

Materials and Methods

Cell Culture, Reagents and Treatments

All the chemicals were obtained from Sigma (St Louis, MO, USA) unless otherwise specified. BxPC3, HupT3, Panc01, CFPAC-1, L3.6 were obtained from ATCC. Panc01 and CFPAC were maintained in DMEM medium. BxPC3 and HupT3 were maintained in RPMI-1640 medium. L3.6 cells were maintained in MEM medium and supplemented with 1% non-essential MEM amino acids. Pancreatic cancer patient-derived xenografts (PDX) cell lines including 6741, 5160, 6413 and 4041 were developed from PDAC tissue resections that had been established in nude mice as previously described {28} and were maintained in DMEM-F12 medium. GSK-3β-null mouse embryonic fibroblasts (MEFs) and matching wildtype MEFs were a kind gift from Dr. Jim Woodgett (Ontario Cancer Institute, Toronto, ON, Canada) and maintained in DMEM medium. All culture media were supplemented with 10% fetal bovine serum (FBS), 1% L-glutamine and 1% penicillin streptomycin. Cells were counted and plated 24 hours before treatment. Mycoplasma detection kit (Lonza, GA, USA) was used for detecting mycoplasma contamination. The latest testing was performed on April 30th, 2019. All cells used in the described experiments were collected within 5 passages. The GSK-3 inhibitor Bio (Selleckchem, Houston, TX), 9-ING-41 (Actuate Therapeutics Inc., Fort Worth, TX), gemcitabine (Eli Lily, Indianapolis, IN), Irinotecan liposomal formulation (IRT-LP; obtained from the Mayo Pharmacy) and MG132 (Sigma-Aldrich, St. Louis, MO) were also used in this study.

MTS and Clonogenic Assay

Cell proliferation was measured by 3-(4,5-dimethylthiazol-2-yl)-5-(3-carboxymethoxyphenyl)-2-(4-sulfophenyl)-2H-tetrazolium) (MTS) assay (Promega, Madison, WI). Briefly, 5000 cells/well were seeded in a 96-well culture plates and incubated in culture medium with or without indicated drug treatments for 48 hours. Medium was removed, and fresh medium was added to each well along with 1:20 dilution of MTS solution. After 2 hours of incubation, the plates were analyzed with a microplate reader at a wavelength of 490 nm (Molecular Devices, Sunnyvale, CA). To assess for potential drug synergy, the combination index (CI) was calculated using CalcuSyn (Biosoft, Cambridge, United Kingdom). For clonogenic assays, cells were collected and seeded in 6-well plates at 1500 cells/ml. After a 4-hour incubation, which allowed cells to attach, culture medium with or without indicated vehicle or drug treatments were added. 48 hours later, supernatant in the wells were aspirated and washed with PBS (NaCl 0.137 M, KCl 2.7 mM, Na2HPO4 8.1 mM, KH2PO4 1.5 mM, pH 7.4) to remove residual drug. Fresh medium was then added to allow colony formation. Colonies were grown until visible and counted after staining with Coomassie brilliant blue R (42% methanol, 16.8% acetic acid, 1 mg/mL Brilliant blue R).

Subcutaneous and Orthotopic Pancreatic Cancer Animal Model

The evaluation of 9-ING-41 in combination with gemcitabine therapy in patient-derived xenograft (PDX) pancreatic tumor model was carried out in the Center for Developmental Therapeutics, Northwestern University, Evanston, IL as previously described {29}. The pancreatic PDX tumor model PCF 379419 was transplanted subcutaneously into the flanks (left and right side) of nude mice (Jackson Laboratory). Three weeks after tumor transplantation, mice were randomized into four groups (n=3/group) and treated with: Vehicle (DMSO), Gemcitabine (10 mg/kg in week 1 and 5 mg/kg in week 2 and 3), 9-ING-41 (40 mg/kg), or both Gemcitabine and 9-ING-41 twice a week for three weeks by i.p. injection. For orthotopic pancreatic cancer animal models, 6–8 week old NSG male mice were procured from Charles River Laboratories and housed in the institutional animal facilities. All animal experiments had approval from the Institutional Animal Care and Use Committee of the Mayo Clinic. To establish an orthotopic pancreatic tumor model, approximately 1 million 6741 PDX cells suspended in 100 μL PBS containing 20% matrigel were slowly injected orthotopically into the head pancreas. In the orthotopic studies, 9-ING-41 was diluted in PEG400/Tween80/Ethanol (PTE) at a ratio of 75:8:17. Prior to injection, an equal volume of saline was used to further dilute the sample. Three weeks following tumor cell implantation, mice were randomly divided into four groups (n=5) and treated with: Vehicle (vehicle consisted of PTE), Gemcitabine (10 mg/kg), 9-ING-41 (40 mg/kg), or both Gemcitabine (10 mg/kg) and 9-ING-41 (40 mg/kg) twice a week for four weeks by i.p. injection. In the combination group, gemcitabine was given one hour following 9-ING-41 injection. Tumor size was measured with calipers and tumor volume was calculated using the formula $1/2(\text{Length} \times \text{Width}^2)$. At the end of the study, tumors were collected, fixed in 10% formalin and embedded in paraffin. A similar experimental design was used for the survival study in which the PDX cell lines 4535, 4636, 6741, and 4911 were injected orthotopically. In this experiment, the treatment protocol was 2 chemotherapeutic injections per week for 4 weeks. An addition to this experiment was the use of IRT-LP at 15 mg/kg as well as the combination of 9-ING-41 and IRT-LP. Mice were

subsequently monitored and euthanized when IACUC endpoint criteria were reached. The date of death was recorded from the end of last treatment.

Western Blot Analysis

Cells were lysed with Western Lysis Buffer (1% Triton X-100, 10 mM Tris Base, 50 mM NaCl, 5 mM EDTA, 50 mM NaF, 30 mM Na4P2O7 pH 7.4) supplemented with aprotinin, leupeptin, sodium orthovanadate, phenylmethylsulfonyl fluoride (PMSF) and calyculin A (Cell Signaling Technologies, Beverly, MA, USA). Lysates were subjected to sodium dodecyl sulfate (SDS)-polyacrylamide gel electrophoresis and immunoblotting as described {16}. Antibodies used for immunoblotting and immunofluorescence are described in detail in Supplemental Table S1.

siRNA, Plasmid Construction and Transfection

Stealth siRNAs were purchased from Invitrogen (HSS104518 and HSS104519 for GSK-3α; HSS104522 and HSS104523 for GSK-3β) and transfected with Lipofectamine® RNAiMAX reagent (Thermofisher Scientific) according to the manufacturer's instruction. MEF cells were transfected with Lipofectamine 2000 (Invitrogen) according to the manufacturer's instruction. GSK-3β suppression re-expression vectors have been previously described {30}.

Lentiviral packaging transduction and selection of stable cells

Lentivirus packaging, cell infection and selection of pLKO-shRNA stable cells were performed as previously described following institutional biosafety regulations {30}. Briefly, L3.6 and 6741 cells were infected with appropriate amounts of lentiviral particle-containing medium. Twenty-four hours later, virus-containing medium was replaced with fresh medium supplemented with 2 μg/ml of puromycin. Pooled resistant clones were used for experiments.

Cell cycle analysis, induction of cell cycle arrest and EdU labeling

For cell cycle analysis, the treated cells were harvested, washed with PBS, and fixed with precooled 70% ethanol in the dark at −20°C for 1 hour. The fixed cells were then washed with PBS and treated with RNase I at 37°C for 30 mins. Finally, the cells were stained with PI solution (20 μg/ml propidium iodide in 10% sodium citrate with 0.1% Triton X-100) at room temperature for an additional 15 mins and analyzed on a FACSCanto II flow cytometer (BD Bioscience, San Jose, CA). Data were processed using Modfit (Verity Software, Maine, USA). To arrest cell cycle at M phase, asynchronous cells were treated with 2 mM thymidine (Sigma, MO, USA) for 24 hours. Then, the cells were released from the thymidine block for 3 hours by washing once with PBS and adding fresh culture medium. Finally, 100 ng/ml Nocodazole (Sigma, MO, USA) was added to the medium for 12 hours, and M phase-arrested cells were collected by shaking. For EdU (5-ethynyl-2'-deoxyuridine) labeling, cells were treated with EdU at a concentration of 10 μM for 1 hour before harvesting. Staining was performed by Click-iT® EdU Alexa Fluor® 488 Flow Cytometry Kit (Invitrogen, Carlsbad, CA). Cells were trypsinized (Invitrogen, Carlsbad, CA) and resuspended in 0.5% bovine serum albumin in PBS and fixed with 4% paraformaldehyde. Cells were permeabilized and stained using the cocktail mixture outlined and provided by

manufacturer. Stained cells were resuspended and analyzed on the FACSCanto II flow cytometer (BD Bioscience, San Jose, CA), and data were processed using FlowJo (TreeStar, Ashland, OR). The mean fluorescence intensity (MFI) was defined as the geometric mean of the given fluorescent probe.

Cell apoptosis and necrosis analysis

Apoptosis and necrosis of pancreatic cancer cells were measured as described {30}. Briefly, the treated pancreatic cancer cells were detached by trypsinization and stained with annexin V labeled with APC (BD Bioscience, San Jose, CA) and propidium iodide (PI, 20 μg/ml, Sigma) for 15 mins. Cells (50,000 per condition) were then analyzed on the FACSCanto II flow cytometer (BD Bioscience, San Jose, CA) and the fraction of cells positive for annexin V and/or PI was calculated using FlowJo (TreeStar, Ashland, OR).

Immunofluorescence staining

The 6741 PDAC cells were plated on coverslips and left to attach overnight. Cells were subsequently treated as indicated and fixed for IF studies to measure pS317 Chk1, gamma-H2Ax and EdU-488. The percentage of EdU-488 positive cells was enumerated and the nuclear MFI of pS317, gamma-H2Ax and EdU-488 were measured using the ImageJ open source image-processing package. Additionally, FPPE sections from 6741 orthotopic experiments were subjected to immunofluorescence staining for pS317 Chk1 as previously described {16, 31}. The MFI for nuclear pS317 Chk1 was measured using ImageJ. Confocal images were collected with an LSM-800 laser scanning confocal microscope with a 63×-oil Plan-Apochromat objective lens using ZEN Blue 2.6 software package (Carl Zeiss, Oberkochen, Germany).

Statistical analysis

Data are expressed as mean ± SEM and analyzed by repeated measures analysis of variance, one-way ANOVA and unpaired Student’s t-test using GraphPad Prism software (GraphPad Software Inc., La Jolla, CA). A value of $p < 0.05$ denotes statistical significance.

Results

9-ING-41 reduces growth of PDAC cells and sensitizes them to gemcitabine *in vitro*

The novel small-molecule ATP-competitive GSK-3 inhibitor 9-ING-41 has been shown to inhibit various human cancer cells growth *in vitro* and significantly increase tumor-killing effect when combined with chemotherapies in resistant glioblastoma and breast cancer {27, 29, 32, 33}. To examine its anti-tumor proliferation effect on pancreatic cancer cells, 5 previously described PDAC cell lines {30} and 3 recently developed pancreatic cancer PDX {28} cell lines were plated and treated with 9-ING-41 in increasing nanomolar concentrations (50 nM, - 2000 nM). Growth suppression was observed in all tested cell lines using a colorimetric, MTS assay after 48 hours (Figure 1A). We next tested the effect of 9-ING-41 in combination with gemcitabine. While 9-ING-41 alone inhibited 6741 proliferation at both 48 and 72 hours, it also synergistically sensitized 6741 (Figure 1B) and 5160 (Supplemental Figure 1A) to gemcitabine as determined by calculating the combination index. To further investigate the cancer cell killing and chemo-sensitizing effect

of 9-ING-41, we utilized L3.6 and 6741 in a clonogenic assay (Supplemental Figure S1B and C). L3.6 and 6741 colony numbers decreased in a dose-dependent manner following 9-ING-41 treatment (Figure 1C). When combined with increasing doses of gemcitabine, 9-ING-41 could substantially reduce colony number compared to gemcitabine alone (Figure 1D). Previous studies have shown that 9-ING-41 treatment inhibited the proliferation of ovarian cancer cell lines by induction of apoptosis {27}. Therefore, we examined cell apoptosis/necrosis by annexin V/PI staining in 9-ING-41 treated pancreatic cancer cells. As shown in Supplement Figure S2A and S2B, combination of both 9-ING-41 and gemcitabine decreased the number of live cells and increased the population of necrotic cells. Immunoblotting results further confirmed the phenotype of significant cell death in the combination drug group (Supplement Figure S2C). Taken together, these data suggest that 9-ING-41 can suppress cell proliferation and sensitize PDAC cells to gemcitabine *in vitro*.

The combination of 9-ING-41 and gemcitabine limits tumor growth *in vivo*

To better understand the anti-tumor effect of 9-ING-41 alone and in combination with gemcitabine *in vivo*, we first tested 9-ING-41 using the PDAC PDX model PCF379419. As shown in Figure 2A, the PDX tumor expanded aggressively in the vehicle and 9-ING-41-treated animals, whereas monotherapy with gemcitabine suppressed, but didn't completely block tumor growth. In contrast, the combination treatment with 9-ING-41 and gemcitabine caused a profound decrease in tumor growth, ending with notable regression after 3 weeks of treatment (Figure 2A, and B).

We next evaluated the effect of 9-ING-41 using an orthotopic tumor mouse model {34}. The 6741 PDAC cell line was implanted into the head of the pancreas and allowed to grow until tumors were palpable. Mice were then randomized into treatment groups and treated twice a week for 4 weeks (Figure 2C). Two days following the last round of therapy, orthotopic tumors were isolated and tumor weight and volume were measured. Although we did observe a statistically significant inhibition of tumor growth with monotherapy treatment in the orthotopic model when compared to vehicle, consistent with the subcutaneous model, we observed a greater reduction in tumor weight and tumor volume in animals that received combination therapy when compared to either vehicle or monotherapy (Figure 2D). Lastly, we orthotopically implanted 6741 and three additional PDX-derived tumor cell lines (4535, 4636 and 4911) and assessed survival following individual or combination drug treatments. In addition to using gemcitabine, we also used liposomal-formulate irinotecan (IRT-LP) to assess whether 9-ING-41 would also show increased efficacy when combined with this recently approved therapy for PDAC. Following implantation of the tumors, mice were monitored for tumor growth and then randomized and treated twice a week for four weeks (Supplemental Figure 3A). Following the four-week treatment animals were monitored and euthanized when IACUC endpoints were met. All four vehicle-treated animals succumb to their tumors within one-week following treatment, whereas animals treated with 9-ING-41, gemcitabine or IRT-LP monotherapy survived slightly longer and varied by cell line and their sensitivity to gemcitabine or IRT-LP (Supplemental Figure 3B). Combining 9-ING-41 with either gemcitabine or IRT-LP significantly extended survival compared to the monotherapy treatment in all four-cell line models examined (Supplemental Figure 3B).

Taken together, these in vivo studies suggest that PDAC patients may benefit from the combination of 9-ING-41 with existing chemotherapies.

GSK3 inhibition impairs gemcitabine induced Chk1 activation in PDAC cells

We next sought to understand the mechanism by which 9-ING-41 could sensitize PDAC cells to gemcitabine. Since gemcitabine induces the DDR pathway through activation of ATR, we initially investigated the phosphorylation of Chk1 (an ATR target) at S345 following gemcitabine treatment. As expected, gemcitabine treatment induced a time-dependent increase in Chk1 S345 phosphorylation in all cell lines examined (Figure 3A). Consistent with our previous study {26, 27}, 9-ING-41 increased the inhibitory phosphorylation of GSK-3β at serine 9 in pancreatic cancer cells (Supplement Figure S4A). We next investigated whether treatment with 9-ING-41 or a tool compound GSK-3 inhibitor, Bio, could impair gemcitabine-induced phosphorylation of Chk1. Significantly, a 2-hour pretreatment with either 9-ING-41 or Bio abrogated the gemcitabine-induced phosphorylation of Chk1 at both S317 and S345 (Figure 3B and C). Although it has been shown that Chk1 is a negative regulator of polo-like kinase 1 (PLK1) {35}, we only detected a slight change in PLK1 phosphorylation (Supplement Figure S4B). Consistent with activation of Chk1 induced by gemcitabine, cell cycle analysis by PI staining showed significantly increased G1/S and decreased G2/M population in gemcitabine-treated group, while GSK-3 inhibition partially abolished the cell cycle arrest (Supplement Figure S5A). To further evaluate whether GSK-3 inhibition restored cell cycle progression, we monitored EdU incorporation into cells actively synthesizing DNA. While neither vehicle nor GSK-3 inhibitor treatment affected EdU incorporation, as expected, treatment with gemcitabine led to decreased EdU incorporation in all three PDAC cell lines tested (Figure 3D and E and Supplemental Figure S5C and D). In contrast, pretreatment with either GSK-3 inhibitor prevented the gemcitabine-induced S-phase arrest (Figure 3D and E and Supplemental Figure S5C and D). Taken together, these data indicate that GSK-3 inhibition abrogates the activation of the ATR-Chk1 DDR leading to S-phase arrest.

GSK-3β regulates the ATR-Chk1 signaling pathway

Since 9-ING-41 and Bio are not totally selective for GSK-3β or GSK-3α, we next sought to determine which of these two kinases participated in the activation of the ATR-Chk1 pathway. To accomplish this, we depleted GSK-3β or GSK-3α in PDAC cell lines using siRNA and examined the phosphorylation of Chk1 following gemcitabine treatment. As can be seen in Figure 4A, depletion of either GSK-3 kinase led to a reduction in gemcitabine-induced Chk1 phosphorylation, with GSK-3β depletion having a more pronounced effect. Since the effect on Chk1 phosphorylation was impacted more by GSK-3β depletion we next constructed stable GSK-3β knockdown L3.6 and 6741 cells (Figure 4B). Similar to the siRNA knockdown results, depletion of GSK3β showed a significant effect on Chk1 phosphorylation following gemcitabine treatment when compared to shVector control cells (Figure 4B). Consistent with these results, GSK-3β knockout mouse embryonic fibroblasts (MEF) transfected with an empty Flag-Vector exhibited remarkable reduction of phosphorylated Chk1 after gemcitabine treatment compared to wildtype (WT) MEF cells (Figure 4C). Significantly, re-expression of Flag-GSK-3β in GSK-3β knockout cells rescued Chk1 phosphorylation (Figure 4C). Lastly, L3.6 cells engineered to be stably depleted of

GSK-3β and expressing either kinase-dead or constitutively active GSK-3β were assessed for gemcitabine-induced activation of Chk1. As can be seen in Figure 4D and E, stable knockdown of GSK-3β impacted gemcitabine-induced phosphorylation of Chk1, which was not rescued by re-expression of kinase-dead GSK-3β, but was substantially restored in cells expressing constitutively active GSK-3β. Altogether, these data provide genetic evidence that GSK-3β, and to some extent GSK-3α, regulate the gemcitabine-induced DDR signaling pathway leading to ATR-Chk1 activation.

GSK-3 contributes to Chk1 activation through stabilization of TopBP1

ATR-dependent phosphorylation of Chk1 during DNA replication stress depends upon several other signaling proteins including ATR interacting protein (ATRIP), and the trimetric Rad9-Hus1-Rad1 (9–1-1) clamp and topoisomerase llβ binding protein (TopBP1) {36}. To determine the mechanism by which GSK-3 inhibition impacts ATR-Chk1 activation, we examined the protein levels of TopBP1, ATR, and ATRIP following GSK-3 inhibitor treatment. As can be seen in Figure 5A, treatment of PDAC cell lines with either GSK-3 inhibitor did not affect the levels of ATR or ATRIP, but did lead to substantially reduced levels of TopBP1. Moreover, siRNA knockdown of GSK-3β led to a reduction in TopBP1 protein levels (Figure 5B). It has been shown that Claspin is also required for ATR-Chk1 activation downstream of TopBP1 {37}. However, we did not observe any change in Claspin protein levels following GSK-3 inhibitor treatment (Supplement Figure S6A).

It was recently shown that TopBP1 plays a crucial role in the maintenance of genomic integrity through the induction of DNA damage repair pathways {38, 39}. Therefore, we performed immunofluorescent staining of gamma-H2Ax on cells 48 hours following the withdrawal of a 2-hour gemcitabine treatment in the presence or absence of 9-ING-41. Significantly, GSK-3 inhibition increased DNA damage and impaired DNA damage repair in pancreatic cancer cells (Supplement Figure S6B and C). Since it was shown that TopBP1 is degraded in a proteasome-dependent manner {40}, we treated 5160 cells with 9-ING-41 in the presence or absence of the proteasome inhibitor MG132. While 9-ING-41 treatment resulted in a decrease in TopBP1 protein levels, the co-treatment of 9-ING-41 and MG132 rescued TopBP1 protein levels (Figure 5C). Lastly, using the L3.6 reconstituted cell line we found that constitutively active but not kinase-dead GSK-3β could rescue TopBP1 protein levels (Figure 5D). Taken together, these data suggest that GSK-3 kinase activity is required to stabilize the TopBP1 protein.

9-ING-41 decreases pS317 Chk1 levels in gemcitabine-treated animals

We next assessed whether 9-ING-41 could reduce phospho-Chk1 levels in tissues from gemcitabine-treated animals. Initially, we performed EdU incorporation and stained 6741 cells with anti-pChk1 (pS317) that had been treated with control, gemcitabine, 9-ING-41, or combination therapy. Consistent with our immunoblotting and flow cytometry data, phosphorylation of Chk1 at S317 was induced in response to gemcitabine together with dramatic loss of EdU positive cells as compared to DMSO or 9-ING-41 treated cells (Figure 6A and B). Significantly, 6741 cells treated with the combination of 9-ING-41 and gemcitabine showed diminished Chk1 phosphorylation and restored EdU incorporation (Figure 6A and B). We next examined the utility of the pS317 Chk1 antibody in our tissues

harvested from the orthotopic model. Although the tissue staining showed an overall increase in background pS317 staining, gemcitabine treatment led to increased pS317 nuclear staining when compared to vehicle- and 9-ING-41-treated mice (Figure 6C and D). In contrast, animals treated with combination therapy showed lower levels of nuclear pS317 staining. Collectively, these results support the overall mechanism that 9-ING-41 treatment-impairs ATR-mediated activation of the DNA damage response leading to Chk1 phosphorylation.

Discussion

In this study, we have found that the combination of gemcitabine with the clinically relevant small molecule GSK-3 inhibitor, 9-ING-41, impacts PDAC tumor growth *in vitro* and *in vivo* and significantly prolongs survival of mice bearing orthotopic tumors. Mechanistically, we identify a previously unknown role for GSK-3β kinase activity, and to a lesser extent GSK-3α, in the regulation of the ATR-Chk1 DDR signaling pathway through the stabilization of the critical adaptor molecule TopBP1 (Figure 7). These findings suggest that 9-ING-41 should be studied in combination with gemcitabine or liposomal-formulated irinotecan for first line therapy in patients with PDAC. Moreover, our data indicate that 9-ING-41 may overcome gemcitabine resistance in pancreatic cancer.

Although GSK-3β has sometimes been proposed to act as a tumor suppressor in various cancer types through its ability to phosphorylate pro-oncogenic molecules e.g. c-Jun, c-Myc, cyclin D1 and β-catenin, leading to their proteasomal degradation {41}, we and others have previously demonstrated that GSK-3β is overexpressed in many human malignancies including PDAC, and can be targeted for therapeutic intervention {11, 27, 29, 32, 33, 42}. Indeed, in pancreatic cancer, GSK-3 has been implicated in the initiation of pancreatic cancer precursor lesions {16}, resistance to chemotherapy {23} and overexpression correlated with reduced survival {21, 30, 12}. Herein, we show that the combination of 9-ING-41 with gemcitabine can significantly enhance the survival and tumor killing effect *in vivo*. Recently, we have also shown that 9-ING-41 can overcome chemoresistance in breast cancer (33), impair tumor growth in renal cell cancer {32}, neuroblastoma (43), and glioblastoma (29) suggesting that this clinically-relevant compound could be paired with other chemotherapies to treat several different human malignancies.

The DNA damage response pathway is a signaling network that senses different types of damage and coordinates a response that includes activation of transcription, cell cycle control, apoptosis, senescence, and DNA repair {44}. ATR along with its regulator ATRIP sense single-stranded DNA (ssDNA) such as the ssDNA present at stalled replication forks induced by gemcitabine (45). Chk1 is one of the established substrates for ATR that initiates a secondary wave of phosphorylation events that impact signaling networks leading to cell cycle arrest and DNA repair {46}. Several studies have shown that cancer cells lacking ATR or Chk1 are vulnerable to chemotherapeutics including gemcitabine and cytarabine highlighting the possibility that inhibiting the ATR-Chk1 signaling pathway may sensitize tumor cells or overcome resistance to chemotherapies that induce this DNA damage checkpoint {47, 45}. Recently, several studies using ATR or Chk1 inhibitors in combination with gemcitabine provided direct evidence that targeting ATR-Chk1 signaling could

sensitize PDAC cells to gemcitabine {48, 49}. Herein, we observed synergistic tumor killing when 9-ING-41 was combined with gemcitabine or IRT-LP. Surprisingly, we found that GSK-3 inhibition or genetic depletion of GSK-3β blocked the phosphorylation of Chk1 following gemcitabine addition. We further demonstrated that GSK-3β was involved in stabilizing TopBP1, a critical adaptor molecule that is recruited to stalled replication forks and involved in the full activation of ATR {50, 45}. While it is presently unclear how GSK-3β stabilizes TopBP1, our data suggest that it requires a phosphorylation event either directly on TopBP1 itself, or on another protein involved in TopBP1 stability. Regardless of the mechanism, our data provide new insight into the regulation of the TopBP1/ATR/Chk1 signaling cascade and add TopBP1 to the ever-growing list of proteins whose function/stability are regulated by GSK-3β.

In summary, our study identified a heretofore-unknown role for GSK-3β in the regulation of ATR-mediated DDR checkpoint signaling through the stabilization of TopBP1. Moreover, this study provides valuable pre-clinical data for the inclusion of patients with PDAC in studies of 9-ING-41 given in combination with chemotherapy.

Supplementary Material

Refer to Web version on PubMed Central for supplementary material.

Acknowledgements

We would like to thank members of the Division of Oncology Research especially Drs. Scott Kaufmann, Larry Karnitz, Zhenkun Lou as well as members of the Billadeau laboratory for helpful discussions.

Financial support: This work was supported by the Pancreatic Cancer SPORE grant CA102701 to D.D.B., and National Institutes of Health grant CA150190 to D.M.

References

1. Garrido-Laguna I, Hidalgo M. Pancreatic cancer: from state-of-the-art treatments to promising novel therapies. Nat Rev Clin Oncol 2015;12(6):319–34 doi 10.1038/nrclinonc.2015.53. [PubMed: 25824606]
2. Rahib L, Smith BD, Aizenberg R, Rosenzweig AB, Fleshman JM, Matrisian LM. Projecting cancer incidence and deaths to 2030: the unexpected burden of thyroid, liver, and pancreas cancers in the United States. Cancer Res 2014;74(11):2913–21 doi 10.1158/0008-5472.CAN-14-0155. [PubMed: 24840647]
3. American Cancer Society. Cancer Facts & Figures 2019. Atlanta: American Cancer Society; 2019.
4. Burris HA 3rd, Moore MJ, Andersen J, Green MR, Rothenberg ML, Modiano MR, et al. Improvements in survival and clinical benefit with gemcitabine as first-line therapy for patients with advanced pancreas cancer: a randomized trial. J Clin Oncol 1997;15(6):2403–13 doi 10.1200/JCO.1997.15.6.2403. [PubMed: 9196156]
5. Kim MP, Gallick GE. Gemcitabine resistance in pancreatic cancer: picking the key players. Clin Cancer Res 2008;14(5):1284–5 doi 10.1158/1078-0432.CCR-07-2247. [PubMed: 18316544]
6. Conroy T, Desseigne F, Ychou M, Bouche O, Guimbaud R, Becouarn Y, et al. FOLFIRINOX versus gemcitabine for metastatic pancreatic cancer. N Engl J Med 2011;364(19):1817–25 doi 10.1056/NEJMoa1011923. [PubMed: 21561347]
7. Von Hoff DD, Ervin T, Arena FP, Chiorean EG, Infante J, Moore M, et al. Increased survival in pancreatic cancer with nab-paclitaxel plus gemcitabine. N Engl J Med 2013;369(18):1691–703 doi 10.1056/NEJMoa1304369. [PubMed: 24131140]

8. Jia Y, Xie J. Promising molecular mechanisms responsible for gemcitabine resistance in cancer. Genes Dis 2015;2(4):299–306 doi 10.1016/j.gendis.2015.07.003. [PubMed: 30258872]
9. Jope RS, Yuskaitis CJ, Beurel E. Glycogen synthase kinase-3 (GSK3): inflammation, diseases, and therapeutics. Neurochem Res 2007;32(4–5):577–95 doi 10.1007/s11064-006-9128-5. [PubMed: 16944320]
10. Doble BW, Woodgett JR. GSK-3: tricks of the trade for a multi-tasking kinase. J Cell Sci 2003;116(Pt 7):1175–86. [PubMed: 12615961]
11. Ougolkov AV, Fernandez-Zapico ME, Bilim VN, Smyrk TC, Chari ST, Billadeau DD. Aberrant nuclear accumulation of glycogen synthase kinase-3beta in human pancreatic cancer: association with kinase activity and tumor dedifferentiation. Clin Cancer Res 2006;12(17):5074–81 doi 10.1158/1078-0432.CCR-06-0196. [PubMed: 16951223]
12. Ougolkov AV, Fernandez-Zapico ME, Savoy DN, Urrutia RA, Billadeau DD. Glycogen synthase kinase-3beta participates in nuclear factor kappaB-mediated gene transcription and cell survival in pancreatic cancer cells. Cancer Res 2005;65(6):2076–81 doi 10.1158/0008-5472.CAN-04-3642. [PubMed: 15781615]
13. Zhang JS, Koenig A, Harrison A, Ugolkov AV, Fernandez-Zapico ME, Couch FJ, et al. Mutant K-Ras increases GSK-3beta gene expression via an ETS-p300 transcriptional complex in pancreatic cancer. Oncogene 2011;30(34):3705–15 doi 10.1038/onc.2011.90. [PubMed: 21441955]
14. Garcea G, Manson MM, Neal CP, Pattenden CJ, Sutton CD, Dennison AR, et al. Glycogen synthase kinase-3 beta; a new target in pancreatic cancer? Curr Cancer Drug Targets 2007;7(3): 209–15. [PubMed: 17504118]
15. Mishra R Glycogen synthase kinase 3 beta: can it be a target for oral cancer. Mol Cancer 2010;9:144 doi 10.1186/1476-4598-9-144. [PubMed: 20537194]
16. Ding L, Liou GY, Schmitt DM, Storz P, Zhang JS, Billadeau DD. Glycogen synthase kinase-3beta ablation limits pancreatitis-induced acinar-to-ductal metaplasia. J Pathol 2017;243(1):65–77 doi 10.1002/path.4928. [PubMed: 28639695]
17. Kurosu T, Nagao T, Wu N, Oshikawa G, Miura O. Inhibition of the PI3K/Akt/GSK3 Pathway Downstream of BCR/ABL, Jak2-V617F, or FLT3-ITD Downregulates DNA Damage-Induced Chk1 Activation as Well as G2/M Arrest and Prominently Enhances Induction of Apoptosis. Plos One 2013;8(11) doi ARTN e79478 10.1371/journal.pone.0079478.
18. Namba T, Kodama R, Moritomo S, Hoshino T, Mizushima T. Zidovudine, an anti-viral drug, resensitizes gemcitabine-resistant pancreatic cancer cells to gemcitabine by inhibition of the Akt-GSK3beta-Snail pathway. Cell Death Dis 2015;6:e1795 doi 10.1038/cddis.2015.172. [PubMed: 26111057]
19. Meijer L, Skaltsounis AL, Magiatis P, Polychronopoulos P, Knockaert M, Leost M, et al. GSK-3-selective inhibitors derived from Tyrian purple indirubins. Chem Biol 2003;10(12):1255–66. [PubMed: 14700633]
20. Stambolic V, Ruel L, Woodgett JR. Lithium inhibits glycogen synthase kinase-3 activity and mimics wingless signalling in intact cells. Curr Biol 1996;6(12):1664–8. [PubMed: 8994831]
21. Peng Z, Ji Z, Mei F, Lu M, Ou Y, Cheng X. Lithium inhibits tumorigenic potential of PDA cells through targeting hedgehog-GLI signaling pathway. Plos One 2013;8(4):e61457 doi 10.1371/journal.pone.0061457. [PubMed: 23626687]
22. Ban JO, Oh JH, Son SM, Won D, Song HS, Han SB, et al. Troglitazone, a PPAR agonist, inhibits human prostate cancer cell growth through inactivation of NFkappaB via suppression of GSK-3beta expression. Cancer Biol Ther 2011;12(4):288–96. [PubMed: 21613824]
23. Shimasaki T, Ishigaki Y, Nakamura Y, Takata T, Nakaya N, Nakajima H, et al. Glycogen synthase kinase 3beta inhibition sensitizes pancreatic cancer cells to gemcitabine. J Gastroenterol 2012;47(3):321–33 doi 10.1007/s00535-011-0484-9. [PubMed: 22041920]
24. Mamaghani S, Patel S, Hedley DW. Glycogen synthase kinase-3 inhibition disrupts nuclear factor-kappaB activity in pancreatic cancer, but fails to sensitize to gemcitabine chemotherapy. BMC Cancer 2009;9:132 doi 10.1186/1471-2407-9-132. [PubMed: 19405981]
25. Zamek-Gliszczynski MJ, Abraham TL, Alberts JJ, Kulanthaivel P, Jackson KA, Chow KH, et al. Pharmacokinetics, metabolism, and excretion of the glycogen synthase kinase-3 inhibitor LY2090314 in rats, dogs, and humans: a case study in rapid clearance by extensive metabolism

with low circulating metabolite exposure. Drug Metab Dispos 2013;41(4):714–26 doi 10.1124/dmd.112.048488. [PubMed: 23305709]

26. Gaisina IN, Gallier F, Ougolkov AV, Kim KH, Kurome T, Guo S, et al. From a natural product lead to the identification of potent and selective benzofuran-3-yl-(indol-3-yl)maleimides as glycogen synthase kinase 3beta inhibitors that suppress proliferation and survival of pancreatic cancer cells. J Med Chem 2009;52(7):1853–63 doi 10.1021/jm801317h. [PubMed: 19338355]
27. Hilliard TS, Gaisina IN, Muehlbauer AG, Gaisin AM, Gallier F, Burdette JE. Glycogen synthase kinase 3beta inhibitors induce apoptosis in ovarian cancer cells and inhibit in-vivo tumor growth. Anticancer Drugs 2011;22(10):978–85 doi 10.1097/CAD.0b013e32834ac8fc. [PubMed: 21878813]
28. Sagar G, Sah RP, Javeed N, Dutta SK, Smyrk TC, Lau JS, et al. Pathogenesis of pancreatic cancer exosome-induced lipolysis in adipose tissue. Gut 2016;65(7):1165–74 doi 10.1136/gutjnl-2014-308350. [PubMed: 26061593]
29. Ugolkov A, Qiang W, Bondarenko G, Procissi D, Gaisina I, James CD, et al. Combination Treatment with the GSK-3 Inhibitor 9-ING-41 and CCNU Cures Orthotopic Chemoresistant Glioblastoma in Patient-Derived Xenograft Models. Transl Oncol 2017;10(4):669–78 doi 10.1016/j.tranon.2017.06.003. [PubMed: 28672195]
30. Zhang JS, Herreros-Villanueva M, Koenig A, Deng Z, de Narvajas AA, Gomez TS, et al. Differential activity of GSK-3 isoforms regulates NF-kappaB and TRAIL- or TNFalpha induced apoptosis in pancreatic cancer cells. Cell Death Dis 2014;5:e1142 doi 10.1038/cddis.2014.102. [PubMed: 24675460]
31. Ding L, Han L, Dube J, Billadeau DD. WASH Regulates Glucose Homeostasis by Facilitating Glut2 Receptor Recycling in Pancreatic Beta Cells. Diabetes 2018 doi 10.2337/db18-0189.
32. Pal K, Cao Y, Gaisina IN, Bhattacharya S, Dutta SK, Wang E, et al. Inhibition of GSK-3 induces differentiation and impaired glucose metabolism in renal cancer. Mol Cancer Ther 2014;13(2):285–96 doi 10.1158/1535-7163.MCT-13-0681. [PubMed: 24327518]
33. Ugolkov A, Gaisina I, Zhang JS, Billadeau DD, White K, Kozikowski A, et al. GSK-3 inhibition overcomes chemoresistance in human breast cancer. Cancer Lett 2016;380(2):384–92 doi 10.1016/j.canlet.2016.07.006. [PubMed: 27424289]
34. Stephan S, Datta K, Wang E, Li J, Brekken RA, Parangi S, et al. Effect of rapamycin alone and in combination with antiangiogenesis therapy in an orthotopic model of human pancreatic cancer. Clin Cancer Res 2004;10(20):6993–7000 doi 10.1158/1078-0432.CCR-04-0808. [PubMed: 15501979]
35. Tang J, Erikson RL, Liu X. Checkpoint kinase 1 (Chk1) is required for mitotic progression through negative regulation of polo-like kinase 1 (Plk1). Proc Natl Acad Sci U S A 2006;103(32):11964–9 doi 10.1073/pnas.0604987103. [PubMed: 16873548]
36. Cimprich KA, Cortez D. ATR: an essential regulator of genome integrity. Nat Rev Mol Cell Biol 2008;9(8):616–27 doi 10.1038/nrm2450. [PubMed: 18594563]
37. Liu S, Bekker-Jensen S, Mailand N, Lukas C, Bartek J, Lukas J. Claspin operates downstream of TopBP1 to direct ATR signaling towards Chk1 activation. Mol Cell Biol 2006;26(16):6056–64 doi 10.1128/MCB.00492-06. [PubMed: 16880517]
38. Morishima K, Sakamoto S, Kobayashi J, Izumi H, Suda T, Matsumoto Y, et al. TopBP1 associates with NBS1 and is involved in homologous recombination repair. Biochem Biophys Res Commun 2007;362(4):872–9 doi 10.1016/j.bbrc.2007.08.086. [PubMed: 17765870]
39. Jeon Y, Ko E, Lee KY, Ko MJ, Park SY, Kang J, et al. TopBP1 deficiency causes an early embryonic lethality and induces cellular senescence in primary cells. J Biol Chem 2011;286(7):5414–22 doi 10.1074/jbc.M110.189704. [PubMed: 21149450]
40. Blackford AN, Patel RN, Forrester NA, Theil K, Groitl P, Stewart GS, et al. Adenovirus 12 E4orf6 inhibits ATR activation by promoting TOPBP1 degradation. Proc Natl Acad Sci U S A 2010;107(27):12251–6 doi 10.1073/pnas.0914605107. [PubMed: 20566845]
41. Walz A, Ugolkov A, Chandra S, Kozikowski A, Carneiro BA, O'Halloran TV, et al. Molecular Pathways: Revisiting Glycogen Synthase Kinase-3beta as a Target for the Treatment of Cancer. Clin Cancer Res 2017;23(8):1891–7 doi 10.1158/1078-0432.CCR-15-2240. [PubMed: 28053024]

42. Ugolkov AV, Matsangou M, Taxter TJ, O'Halloran TV, Cryns VL, Giles FJ, et al. Aberrant expression of glycogen synthase kinase-3beta in human breast and head and neck cancer. Oncol Lett 2018;16(5):6437–44 doi 10.3892/ol.2018.9483. [PubMed: 30405781]
43. Ugolkov AV, Bondarenko GI, Dubrovskyi O, Berbegall AP, Navarro S, Noguera R, et al. 9-ING-41, a small-molecule glycogen synthase kinase-3 inhibitor, is active in neuroblastoma. Anticancer Drugs 2018;29(8):717–24 doi 10.1097/CAD.0000000000000652. [PubMed: 29846250]
44. Zhou BB, Elledge SJ. The DNA damage response: putting checkpoints in perspective. Nature 2000;408(6811):433–9 doi 10.1038/35044005. [PubMed: 11100718]
45. Lecona E, Fernandez-Capetillo O. Targeting ATR in cancer. Nat Rev Cancer 2018;18(9):586–95 doi 10.1038/s41568-018-0034-3. [PubMed: 29899559]
46. Matsuoka S, Ballif BA, Smogorzewska A, McDonald ER 3rd, Hurov KE, Luo J, et al. ATM and ATR substrate analysis reveals extensive protein networks responsive to DNA damage. Science 2007;316(5828):1160–6 doi 10.1126/science.1140321. [PubMed: 17525332]
47. Karnitz LM, Flatten KS, Wagner JM, Loegering D, Hackbarth JS, Arlander SJ, et al. Gemcitabine-induced activation of checkpoint signaling pathways that affect tumor cell survival. Mol Pharmacol 2005;68(6):1636–44 doi 10.1124/mol.105.012716. [PubMed: 16126823]
48. Koh SB, Courtin A, Boyce RJ, Boyle RG, Richards FM, Jodrell DI. CHK1 Inhibition Synergizes with Gemcitabine Initially by Destabilizing the DNA Replication Apparatus. Cancer Res 2015;75(17):3583–95 doi 10.1158/0008-5472.CAN-14-3347. [PubMed: 26141863]
49. Wallez Y, Dunlop CR, Johnson TI, Koh SB, Fornari C, Yates JWT, et al. The ATR Inhibitor AZD6738 Synergizes with Gemcitabine In Vitro and In Vivo to Induce Pancreatic Ductal Adenocarcinoma Regression. Mol Cancer Ther 2018;17(8):1670–82 doi 10.1158/1535-7163.MCT-18-0010. [PubMed: 29891488]
50. Kumagai A, Lee J, Yoo HY, Dunphy WG. TopBP1 activates the ATR-ATRIP complex. Cell 2006;124(5):943–55 doi 10.1016/j.cell.2005.12.041. [PubMed: 16530042]

Statement of Translational Relevance

Pancreatic ductal adenocarcinoma (PDAC) is a genetically heterogeneous, incurable, intensely chemoresistant malignancy. Glycogen synthase kinase 3β (GSK3β) is an emerging therapeutic target in a spectrum of human malignancies, including PDAC. The data presented herein demonstrate a previously uncharacterized role for GSK3β in the regulation of the TopBP1/ATR/Chk1 DNA damage response pathway. Treatment with the GSK-3 inhibitor 9-ING-41 sensitized PDAC cells to gemcitabine, as well as liposomal irinotecan *in vivo*. As 9-ING-41 has recently entered clinical studies, our data highlight not only a novel mechanism of action for 9-ING-41, but also provide a compelling rationale for the inclusion of patients with PDAC in clinical studies of 9-ING-41 in combination with gemcitabine/abraxane or MM398. These data also support the study of 9-ING-41 with other agents that induce an ATR-mediated DNA damage response.

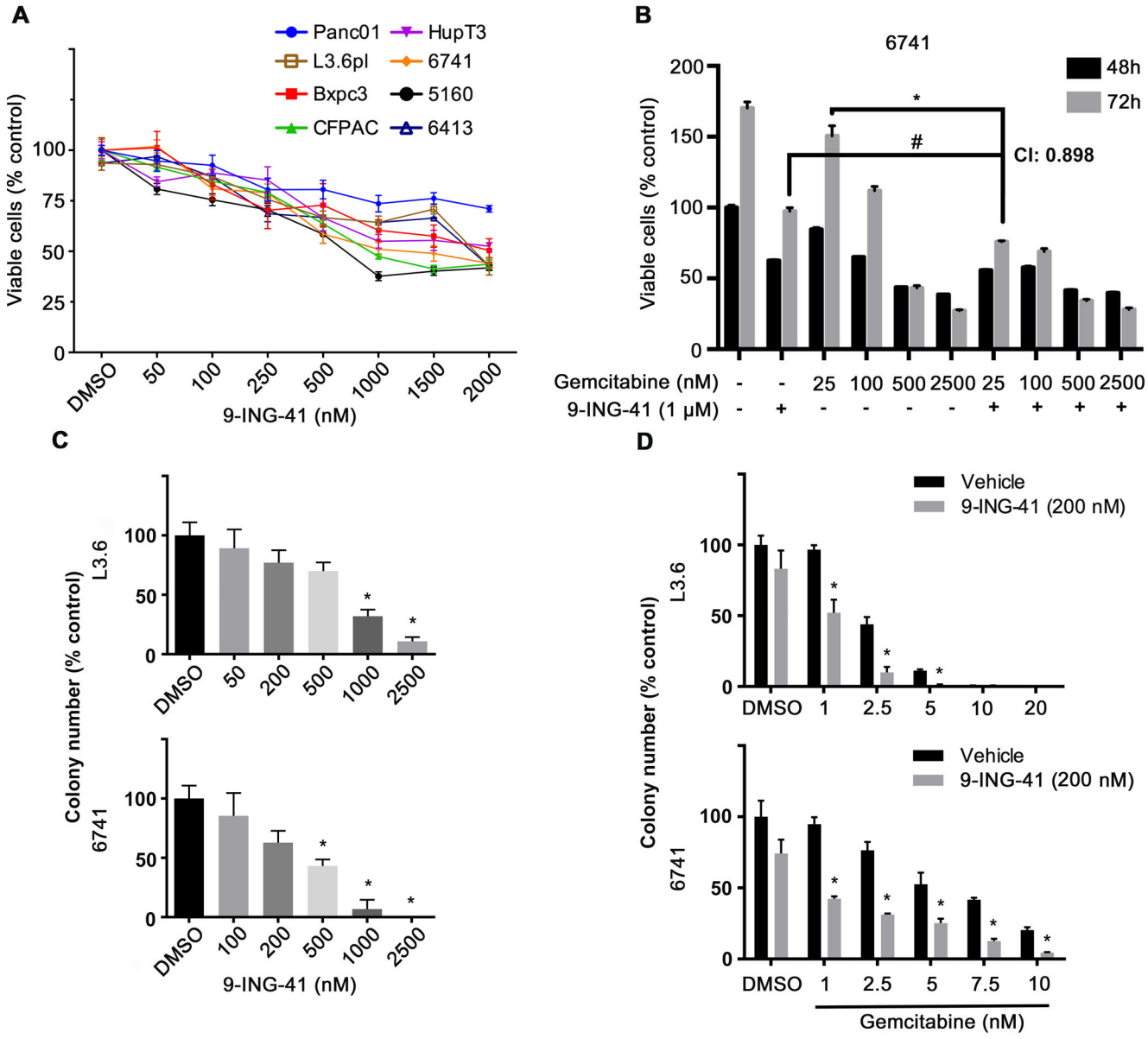

Figure 1. 9-ING-41 treatment synergizes with gemcitabine to abrogate PDAC cell proliferation and colony formation *in vitro*.

(A) The indicated PDAC cell lines were seeded in 96-well plates and treated with DMSO or increasing concentration of 9-ING-41 (nM) for 48 hours. Cell proliferation was determined by MTS assay. Data were quantified as percentage of control and expressed as mean ± SEM. n=6. (B) The 6741 PDX-derived cell line was plated and treated with 1 μM 9-ING-41 alone or with increasing concentrations of gemcitabine (nM) for 48 and 72 hours. Cell proliferation was determined by MTS assay. Data was quantified as percentage of control and expressed as mean ± SE. *P<0.05 gemcitabine and 9-ING-41 combinations versus gemcitabine alone. #P<0.05 gemcitabine and 9-ING-41 combination versus 9-ING-41. CI: combination index. n=6. (C) L3.6 and 6741 PDAC cells were seeded in 6-well plate and treated with DMSO or increasing concentration of 9-ING-41 (nM) for 48 hours. Supernatant

was then removed and remaining cells were allowed to form colonies. Colony number from triplicate samples were counted and expressed as mean ± SEM. *P<0.05 9-ING-41 versus DMSO. (D) Clonogenic assay was carried out as described in (C) but 200 nM 9-ING-41 was added together with increasing concentration of gemcitabine. Colony number from triplicate samples were counted and expressed as mean ± SEM. *P<0.05 gemcitabine and 9-ING-41 combination versus gemcitabine alone.

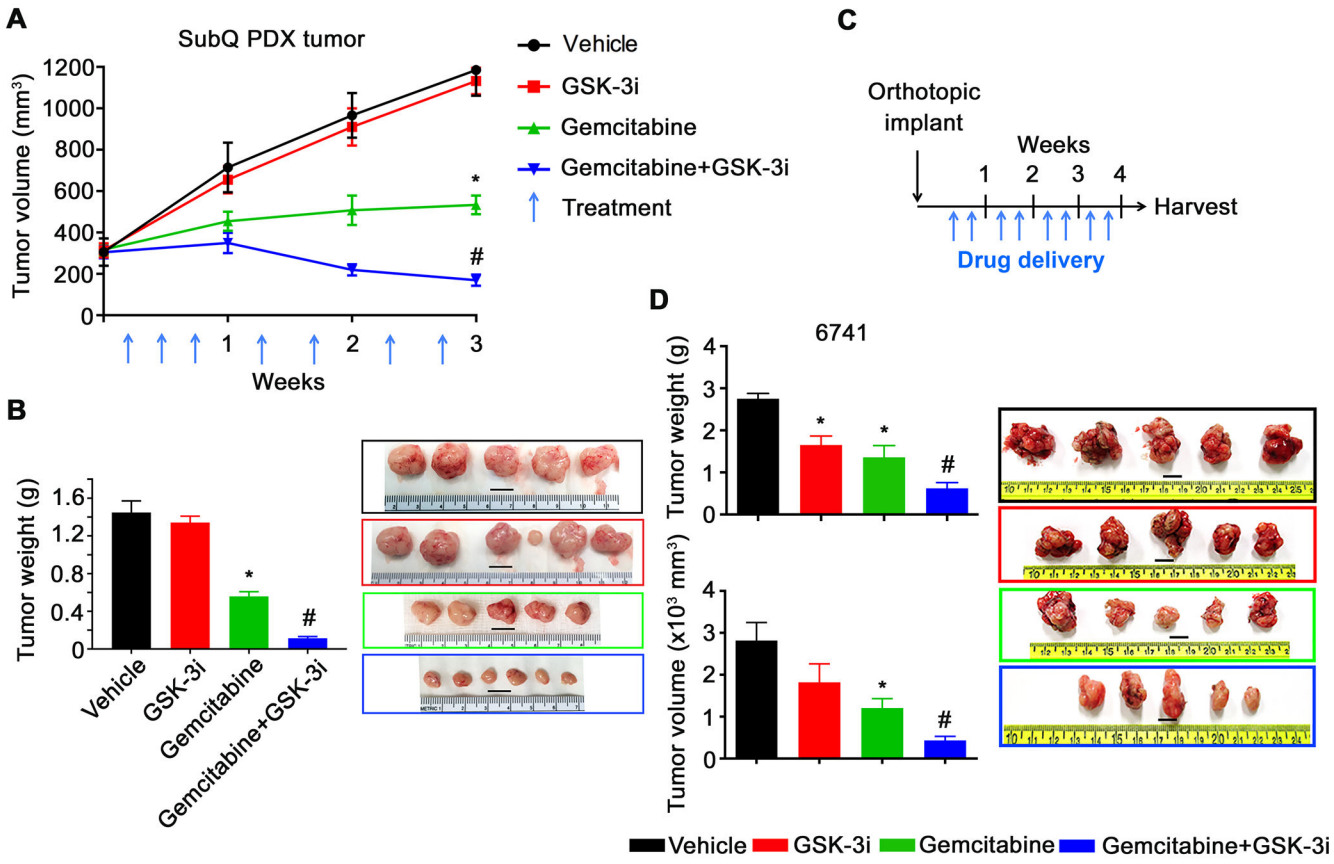

Figure 2. 9-ING-41 and Gemcitabine abrogate tumor growth *in vivo*.

(A) The pancreatic PDX tumor (PCF 379419) was transplanted subcutaneously into both flanks of athymic nude mice (12 mice in total). Tumors were size matched and mice were randomized into 4 treatment groups: Vehicle, Gemcitabine, 9-ING-41 (40 mg/kg) and Gemcitabine + 9-ING-41. Gemcitabine was used as 10 mg/kg (week 1) and 5 mg/kg (week 2 and 3). Vehicle or drugs were injected i.p. Tumor volume was measured weekly and shown as mean ± SEM. (n=3/group). *P<0.05 gemcitabine versus vehicle, #P<0.01 9-ING-41 + gemcitabine versus gemcitabine alone. (B) Tumors were removed and weighed at the end of the study and representative images of the PDX tumors from each group of animals are shown. *P<0.05 gemcitabine versus vehicle, #P<0.05 9-ING-41 + gemcitabine versus gemcitabine alone. The weight of resected tumors were shown as mean ± SEM. One tumor from each of the vehicle, 9-ING-41 and gemcitabine treatment groups did not grow and was thus excluded from the analysis. Bar, 1 cm. (C) Three weeks following orthotopic implantation of 6741 cells into the head of the pancreas, mice were randomly divided into four groups (n=5/group) and treated with the indicated drugs {Vehicle, Gemcitabine (10 mg/kg), 9-ING-41 (40 mg/kg) and Gemcitabine + 9-ING-41} by i/p. injection twice per week for four weeks as shown. (D) At the end of week 4, tumors were removed and tumor weight and tumor volume were measured. *P<0.05 gemcitabine or 9-ING-41 monotherapy versus vehicle, #P<0.05 9-ING-41 + gemcitabine versus gemcitabine alone. Images of the resected tumors are shown. Data was expressed as mean ± SEM. n=5. Bar, 1 cm.

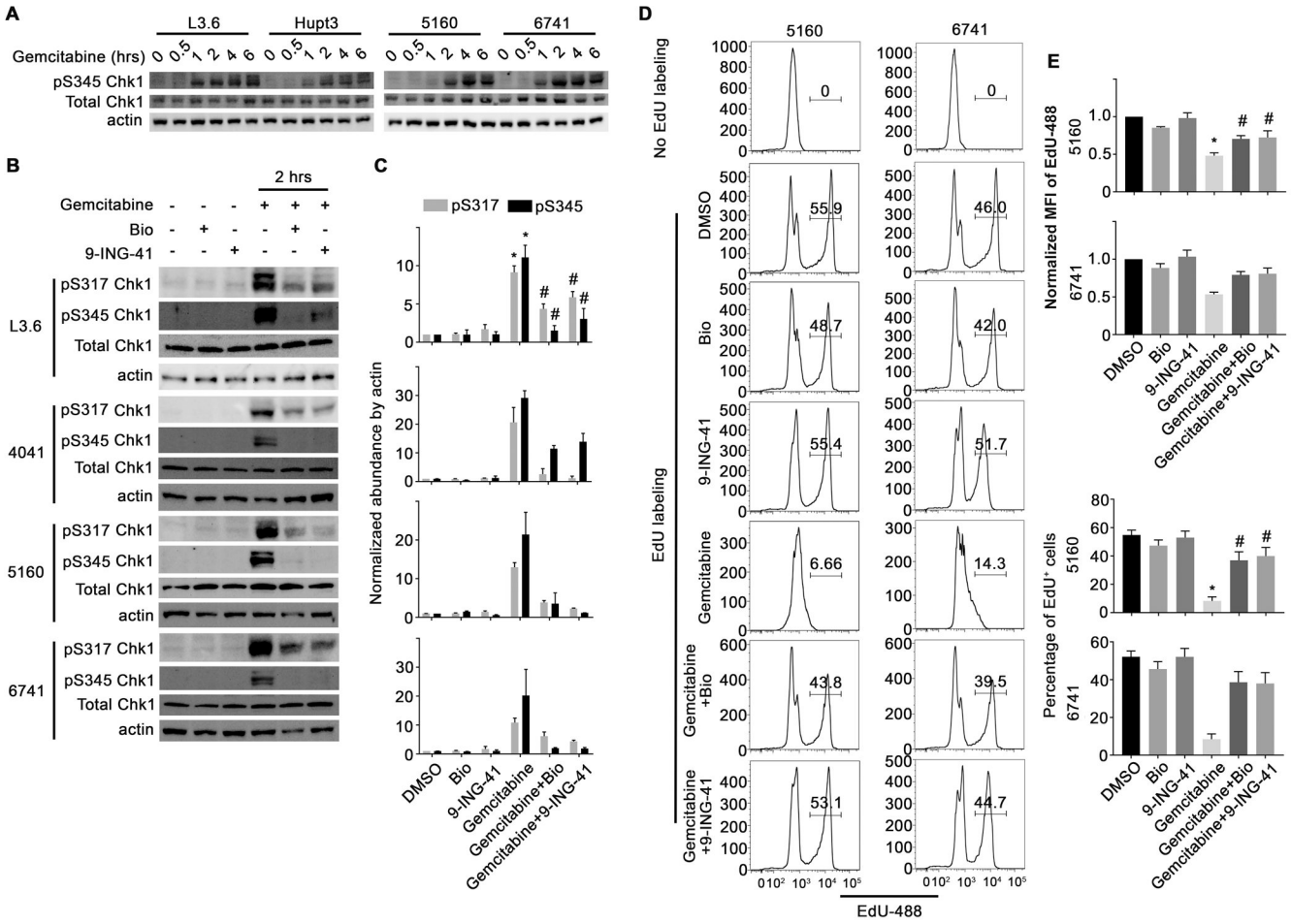

Figure 3. GSK-3 abrogates gemcitabine-induced Chk1 activation and cell cycle arrest.

(A) PDAC cell lines were treated with gemcitabine (500 nM) over the indicated time course, harvested and lysates were prepared and immunoblotted with the indicated antibodies. (B) PDAC cell lines were pretreated with GSK-3 inhibitors Bio (5 μM) or 9-ING-41 (5 μM) for 2 hours followed by an additional 2 hour treatment with gemcitabine (500 nM). Phosphorylated Chk1 at S317 and S345 Chk1, as well as total Chk1 were examined by immunoblotting. β-actin was used as a loading control. (C) Average signal intensity of pS317 and pS345 Chk1 were analyzed and expressed as mean ± SEM. *P<0.05 gemcitabine versus DMSO. #P<0.05 gemcitabine and 9-ING-41 versus gemcitabine alone. Data are representative of three independent experiments. (D) 5160 and 6741 were treated as indicated in Figure 3B and then provided EdU for 1 hour prior to harvesting. EdU incorporation was detected using the EdU detection kit followed by flow cytometry. (E) EdU positive cells were gated and the MFI of the EdU peak is graphically displayed. (E) The normalized Mean fluorescent intensity (MFI) and percentage of EdU-488 positive cells were quantified and expressed as mean ± SEM. *P<0.05 gemcitabine versus DMSO. #P<0.05 gemcitabine and GSK-3 inhibitor versus gemcitabine alone. Data presented in D and E is representative of three independent experiments.

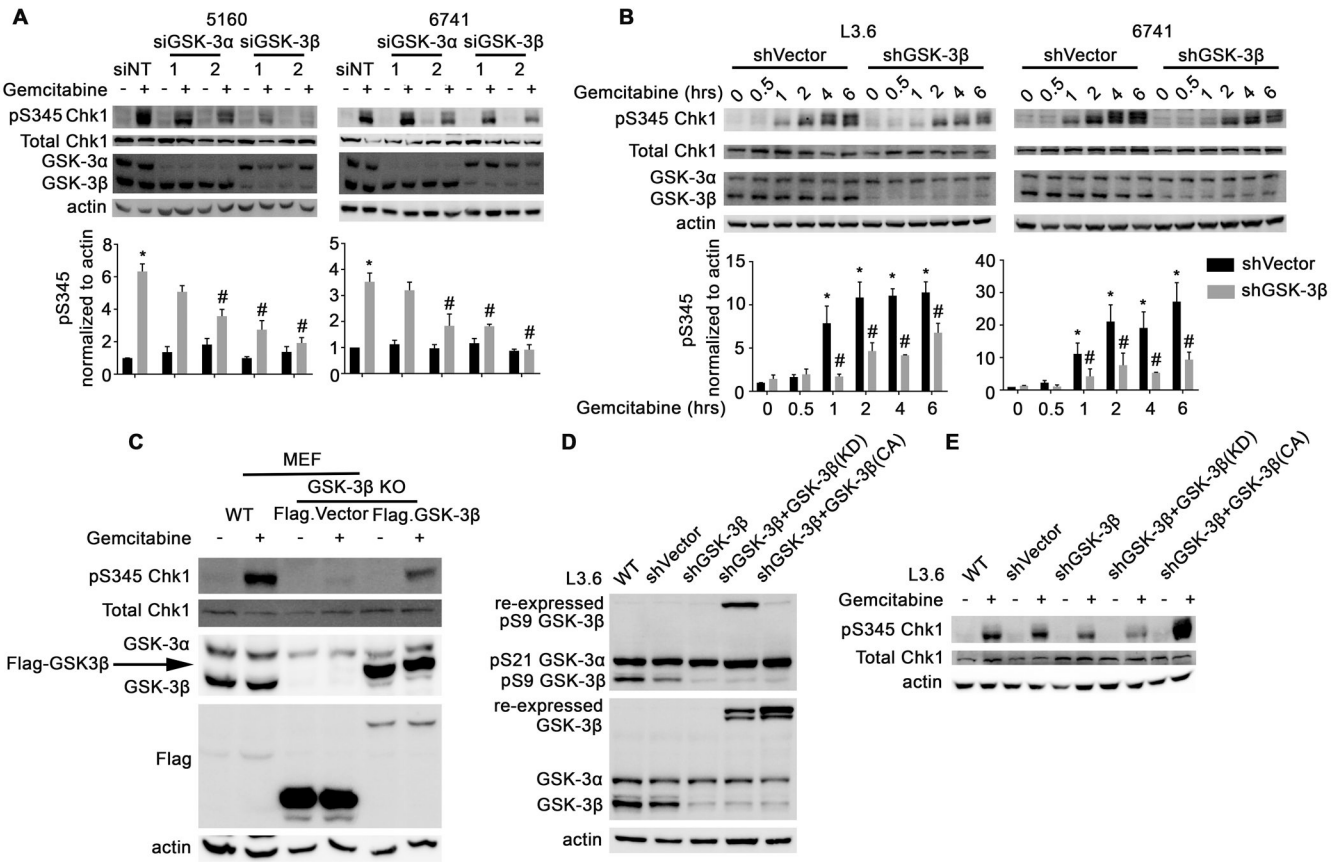

Figure 4. GSK-3β regulates ATR-dependent phosphorylation of Chk1 in response to gemcitabine treatment.

(A) PDAC cell lines were depleted of GSK-3α or GSK-3β using siRNA and then treated with gemcitabine (500 nM) for 2 hours. Cell lysates were prepared and immunoblotted with the indicated antibodies. Average signal intensity of pS345 Chk1 was analyzed and expressed as mean ± SEM. *P<0.05 gemcitabine versus DMSO. #P<0.05 siGSK-3 versus siNT after gemcitabine. n=3. (B) L3.6 and 6741 PDAC cell lines stably depleted of GSK-3β were treated with gemcitabine (500 nM) for 2 hours. Protein lysates were prepared and immunoblotted as indicated. Average signal intensity of pS345 Chk1 was analyzed and expressed as mean ± SEM. *P<0.05 gemcitabine versus DMSO in shVector cells. #P<0.05 shGSK-3β versus shVector cells after gemcitabine. n=3. (C) WT or GSK-3β KO MEFs were left untransfected or transfected with vector control or WT GSK-3β and treated with gemcitabine (500 nM) for 2 hours. Protein lysates were prepared and immunoblotted as indicated. (D and E) L3.6 cells were left uninfected or were infected with a control lentivirus or one that stably depletes GSK-3β and re-expresses a non-targetable kinase-dead or constitutively active GSK-3β cDNA. Cells were then treated with gemcitabine (500 nM) for 2 hours, protein lysates were obtained and immunoblotted as indicated.

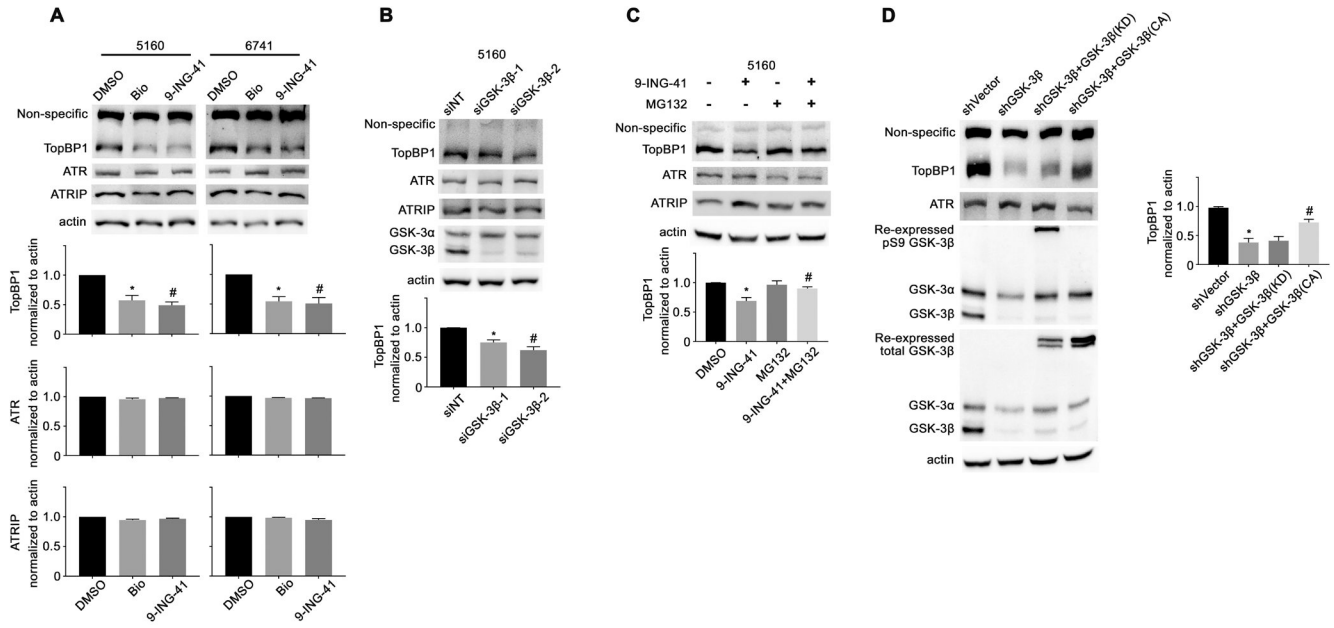

Figure 5. GSK-3β regulates TopBP1 protein stability.

(A) 5160 and 6741 cell lines were treated with the GSK-3 inhibitors Bio (5 μM) and 9-ING-41 (5 μM) for 4 hours. Protein lysates were prepared and immunoblotted with the indicated antibodies. The average signal intensity of TopBP1, ATR and ATRIP were analyzed and expressed as mean ± SEM. *P<0.05 Bio versus DMSO. #P<0.05 9-ING-41 versus DMSO. n=3. (B) Protein lysates were prepared from 5160 cells transfected with control siRNA or siRNA targeting GSK-3β and immunoblotted with the indicated antibodies. The average signal intensity of TopBP1 was analyzed and expressed as mean ± SEM. *P<0.05 siGSK-3β−1 versus siNT. #P<0.05 siGSK-3β−2 versus siNT. n=3. (C) The 5160 cell line was treated with 9-ING-41 (5 μM) with or without MG132 (10 μM) for 4 hours. Cell lysates were prepared and immunoblotted with the indicated antibodies. The average signal intensity of TopBP1 was analyzed and expressed as mean ± SEM. *P<0.05 9-ING-41 versus DMSO. #P<0.05 9-ING-41 and MG132 combination versus 9-ING-41. n=3. (D) Cell lysates were prepared from the panel of L3.6 cell lines described in Figure 4D and immunoblotted with the indicated antibodies. The average signal intensity of TopBP1 was analyzed and expressed as mean ± SEM. *P<0.05 shGSK-3β versus shVector cells. #P<0.05 shGSK-3β with GSK-3β (CA) versus shGSK-3β cells. n=3.

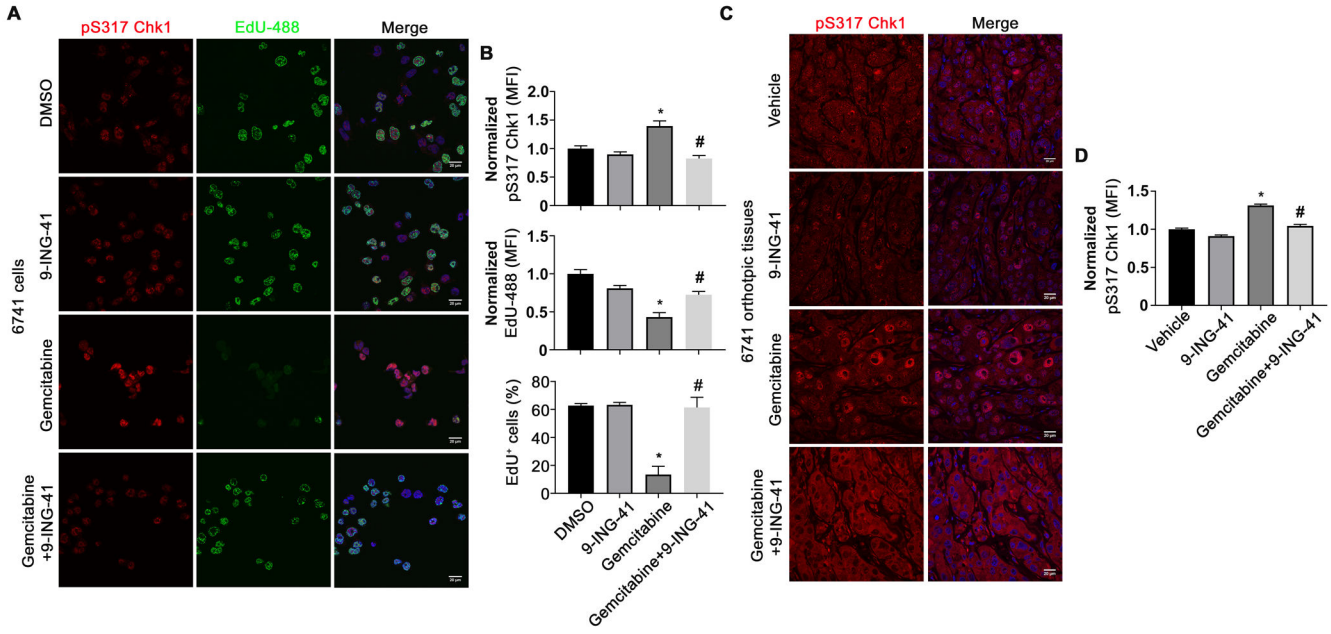

Figure 6. 9-ING-41 reverses Chk1 phosphorylation induced by gemcitabine treatment.

(A) 6741 cells were grown on coverslips, treated with DMSO, 9-ING-41 (5 μM), gemcitabine (500 nM) or the combination of 9-ING-41 and gemcitabine and pulsed with EdU one hour prior to fixation. Fixed cells were subsequently stained with anti-pS317 Chk1 antibodies and detected with an Alexa 568 conjugated donkey-anti-rabbit secondary (red) and EdU-488 (green). DNA was visualized following Hoechst staining (blue). (B) The normalized MFI of nuclear pS317 Chk1, EdU-488 and the percentage of EdU positive cells were evaluated by ImageJ and expressed as mean ± SEM. *P<0.05 gemcitabine versus DMSO. #P<0.05 gemcitabine and 9-ING-41 versus gemcitabine alone. n=200 cells per treatment group. (C) Immunofluorescence staining of pS317 Chk1 (red) and Hoechst (blue) from orthotopic 6741 PDX tumor tissue sections treated as described in Figure 2D. (D) The normalized MFI of pS317 Chk1 within the nucleus was evaluated by ImageJ and expressed as mean ± SEM. *P<0.05 gemcitabine versus Vehicle. #P<0.05 gemcitabine and 9-ING-41 versus gemcitabine. n=200 cells per treatment group.

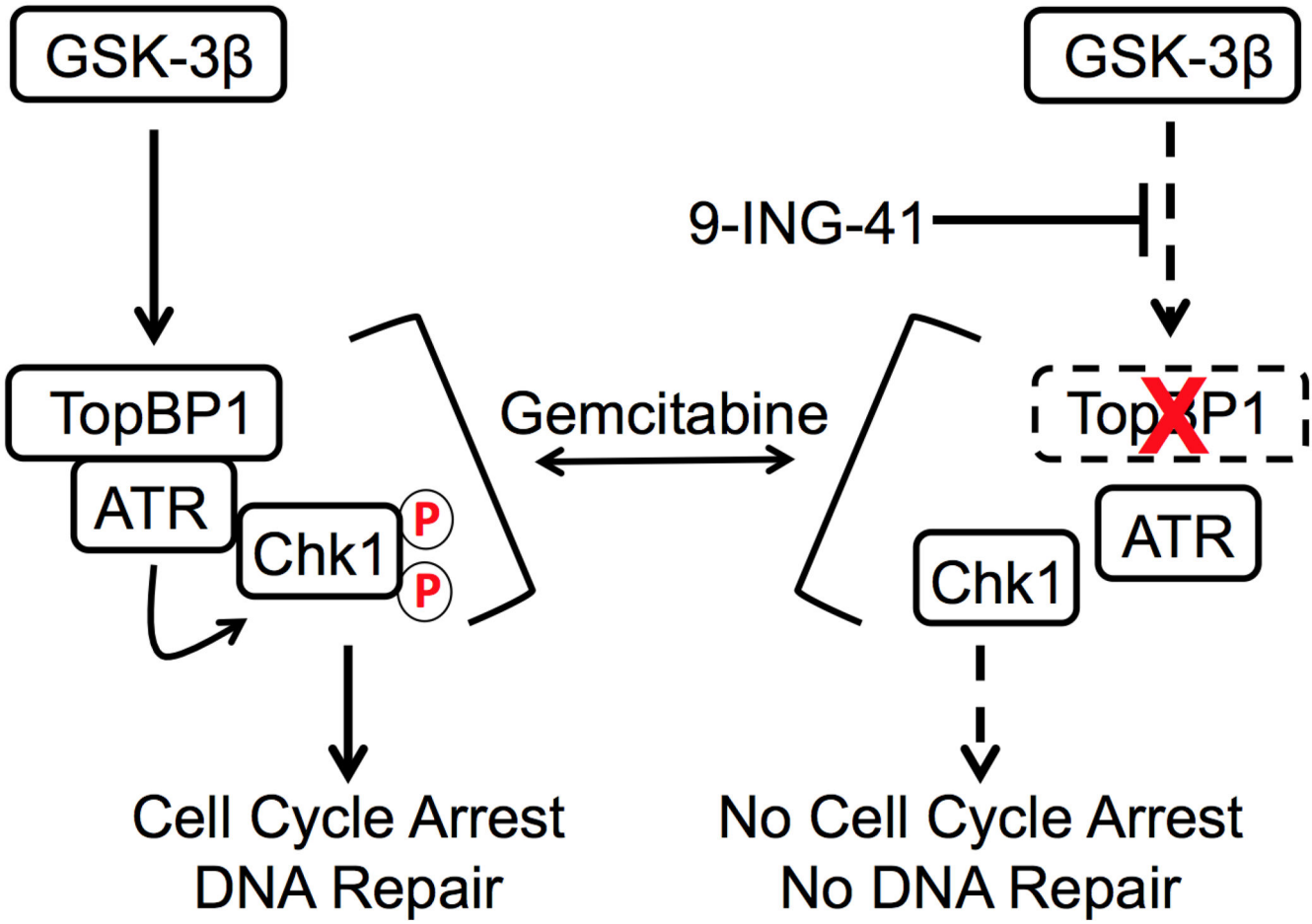

Figure 7. Proposed model by which GSK-3 inhibition by 9-ING-41 disrupts the TopBP1/ATR/Chk1 pathway.

In response to gemcitabine-induced DNA replication stress, TopBP1/ATR/ATRIP (not shown) complexes are recruited to stalled replication forks where ATR can fully activate Chk1 leading to cell cycle arrest and DNA repair. In the presence of 9-ING-41, TopBP1 protein levels are destabilized thus abrogating the full activation of ATR leading to reduced Chk1 phosphorylation and ultimately impaired cell cycle arrest and likely DNA repair. Circle with red P indicates phosphorylation. Dashed rectangle with red X indicates TopBP1 degradation.